Nucleate Pool Boiling Regimes Of Power Electronics Cooling

Ilya T'Jollyn
[1]Department of Electromechanical, Systems and Metal Engineering
Ghent University
Ghent, Belgium
[2]FlandersMake@UGent – Core lab EEDT-MP
Leuven, Belgium
ORCID: 0000-0003-3151-260X

Jasper Nonneman
[1]Department of Electromechanical, Systems and Metal Engineering
Ghent University
Ghent, Belgium
[2]FlandersMake@UGent – Core lab EEDT-MP
Leuven, Belgium
ORCID: 0000-0001-6196-3757

Wim Beyne
Department of Electromechanical, Systems and Metal Engineering
Ghent University
Ghent, Belgium
ORCID: 0000-0002-7450-9382

Michel De Paepe
[1]Department of Electromechanical, Systems and Metal Engineering
Ghent University
Ghent, Belgium
[2]FlandersMake@UGent – Core lab EEDT-MP
Leuven, Belgium
ORCID: 0000-0003-0233-0719

***Abstract*—The boiling curve of refrigerant FK-649 at a saturation temperature of 36°C is experimentally determined for nucleate pool boiling on the baseplate of an IGBT power module. The nucleate pool boiling curve can be subdivided in three zones. At low heat fluxes (lower than 20 kW/m²), partial nucleate boiling occurs. This zone is followed by fully developed nucleate boiling, between 20 kW/m² and 90 kW/m², with a significantly steeper slope of the boiling curve. At even higher heat fluxes, between 90 kW/m² and the critical heat flux, the partial dryout zone results in a decrease of the slope of the boiling curve. A single power-max relation is not appropriate to describe this behaviour, although it is found in the most-used correlations for nucleate pool boiling heat transfer. This work proposes a combination of three power-law relations to fit the measurement data, one for each of the three nucleate pool boiling zones.**

Keywords—electronics cooling, power electronics, heat transfer, nucleate pool boiling, boiling regimes, boiling curve

I. INTRODUCTION

Boiling heat transfer is investigated to enhance cooling of (power) electronics as it exhibits high heat transfer coefficients [1]. Typically nucleate boiling is used, as due to the bubble formation and dynamics at the heated surface, high heat transfer coefficients can be attained. Circulation of the fluid can be achieved by buoyancy of the vapour bubbles (pool boiling) or can be externally forced (flow boiling). Heat transfer in flow boiling is usually modelled as a combination of nucleate pool boiling heat transfer and forced convective heat transfer [2].

Heat transfer in pool boiling is characterized by the boiling curve. The boiling curve is the relation between surface heat flux and surface superheat temperature. The surface superheat temperature is defined as the difference between the surface temperature and the fluid saturation temperature. A typical boiling curve for water describing the different boiling regimes is given in Fig. 1. The nucleate boiling regime, which is of interest for this paper, ranges from A to D. A is the onset of boiling, at lower heat fluxes, heat is transferred through natural convection. At D, dryout occurs at the critical heat flux (CHF). The nucleate boiling regime (between onset of nucleate boiling and critical heat flux) can be subdivided in three zones with distinctly different slopes and flow behaviour, indicated in Fig. 1 by the sections A to B, B to C and C to D. Several researchers, for example [3], refer to the first two zones as partial nucleate boiling (A-B) and fully developed nucleate boiling (B-C). The third zone from C to D does not have a commonly used name, it is referred to here as the partial dryout zone.

The different nucleate boiling regimes been reported and/or measured by several researchers. Kandlikar and Chung [4] describe the three regions similarly to the previous paragraph when explaining the general boiling curve. El-Genk and Bostanci [5] performed measurements on pool boiling heat transfer of refrigerant HFE 7100. Based on the measurement results, they describe the three nucleate boiling regimes at low, intermediate and high surface superheat with different slopes. The measurements shown by Kutateladze [6] for pool boiling of various fluids also indicate three regions with distinctly different slopes on a logarithmic plot. Dhir [3] mentions that a small change in the slope of the boiling curve

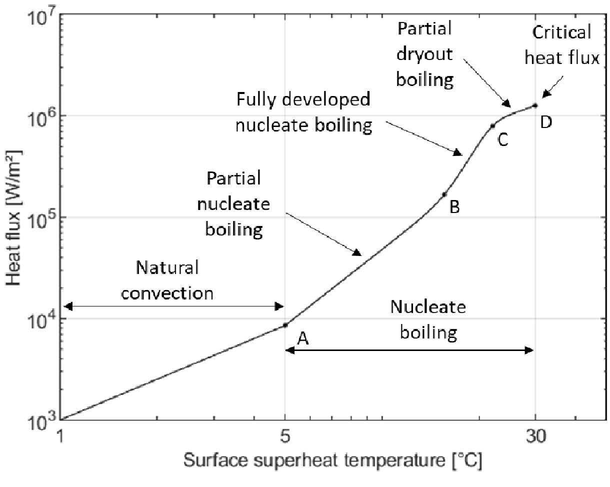

Fig. 1. Pool boiling curve of water showing different boiling regimes (partly adapted from [4]).

can occur upon transition from partial to fully developed nucleate boiling. Forrest et al. [7] did measurements on refrigerants FK-649 and R134a. The measurements of the heat transfer coefficient show a drop at the highest heat fluxes, indicating the transition to critical heat flux. Ji et al. [8] performed measurements with R134a in the intermediate and high heat flux nucleate boiling regions. They compared the measurements with the prediction by the Cooper correlation and concluded that above 250 kW/m², the slope of the boiling curve decreases and the correlation no longer adequately predicts the heat transfer rate.

Many correlations have been proposed to describe the boiling curve in the nucleate boiling regime [9]. Some of the most cited ones are proposed by the following authors (in chronological order): Kruzhilin [10], Rohsenow [11], Forster-Zuber [12], Kutateladze-Borishanskii [13], Borishanksii-Mostinski [14, 15], Shekriladze-Ratiani [16, 17], Labuntsov [18], Gorenflo [19, 20], Stephan-Abdelsalam [21], Cooper [22], Kutateladze [6], Leiner [23] and Pioro [24]. These correlations are based on very different methods and use a multitude of different parameters and fluid properties. All these correlations do have in common that they describe the relation between heat flux $\dot{q}$ and surface superheat temperature ΔT_s as a power law, as in Eq. (1):

$$\dot{q} \sim \Delta T_s^n \qquad (1)$$

The exponent n in this equation varies from 3 to 3.33 in most of these correlations. This power-law relation is not able to represent the three nucleate boiling regimes as shown in Fig. 1.

This paper presents measurements of the boiling curve of FK-649 (also known as Novec-649), to investigate in detail the boiling curve and the different nucleate boiling regimes.

II. Experimental Setup

The boiling curve is measured for heat transfer from the copper baseplate of a IGBT (insulated-gate bipolar transistor) module to refrigerant FK-649. Heating is provided by forcing a DC current through the IGBTs of the module. The baseplate is placed horizontally and the surface in contact with the fluid has a length of 108 mm, a width of 47 mm and an arithmetic mean surface roughness of 0.2 µm.

The refrigerant is contained in a stainless steel reservoir which is shown in Fig. 2 (CAD drawing) and Fig. 3 (picture). The power module is connected to the bottom plate, which is made out of POM (polyoxymethylene) thermoplastic. This material has a lower conductivity than stainless steel, to avoid parasitic heat flows from the module to the refrigerant. Liquid refrigerant evaporates at the baseplate and the generated vapour rises to the top of the reservoir. At the top, the refrigerant condenses on a copper spiral tube. This is achieved by pumping a water-glycol mixture at a temperature below the refrigerant saturation temperature through the spiral condenser. The reservoir is leak-tight, such that the saturation pressure and corresponding saturation temperature of the refrigerant can be varied. In this study, the saturation temperature is kept constant at 36 °C (within 0.5 °C) by varying the water-glycol inlet temperature. The reservoir is insulated by a layer of polyurethane with a thickness of 5 cm and thermal conductivity of 0.025 W/mK (not shown on Fig. 2 and Fig. 3).

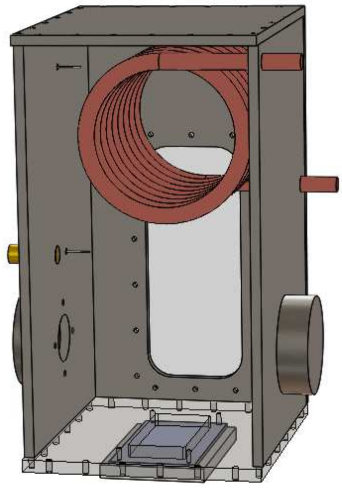

Fig. 2. CAD drawing of the refrigerant reservoir without front plate and insulation.

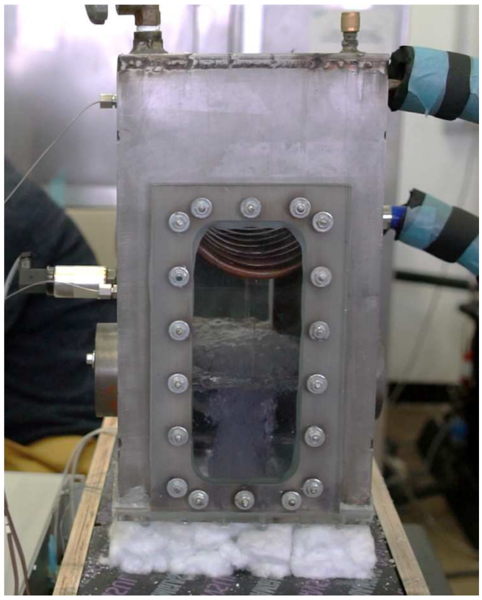

Fig. 3. Picture of the refrigerant resevoir without insulation.

The heat flux is determined by measuring the voltage and current applied to the power module and by dividing with the boiling surface area. The baseplate temperature is measured by three type K mineral insulated thermocouples. The saturation temperature is measured by a type T mineral insulated thermocouple in the reservoir. To analyse heat losses from to the environment, the energy transferred from the reservoir by the water-glycol mixture (also called the net efflux) is also measured. Type T mineral insulated thermocouples measure the inlet and outlet temperature. The volumetric flow rate is measured by an oval gear flow meter. The water-glycol mixture has a mass fraction of 38.24% ethylene glycol and its density and enthalpy is determined with the open-source thermophysical property library CoolProp [25].

The used sensors and their uncertainties are summarized in Table I.

TABLE I. SENSOR UNCERTAINTIES

Sensor	Uncertainty
Current	± 0.24 A
Voltage	± 50 µV ± 0.003%
Thermocouple	± 0.07 °C
Flow rate	± 1.5%

III. RESULTS

A. Energy Balance

To assess how much of the dissipated energy in the IGBT's is transferred to the refrigerant and subsequently the water-glycol coolant circuit, the energy balance of the system is analysed. Fig. 4 shows the dissipated electrical power on the x-axis and the net efflux of energy by the water-glycol flow on the y-axis. The maximal discrepancy is 20 W, indicating that the heat losses are small compared to the heat dissipation (ranging from 50 W to 600 W).

In Fig. 5, the deviation on the energy balance is shown as a function of the boiling surface heat flux. At lower heat fluxes (< 40 kW/m²), the relative deviation is higher than 5%. This is due to the lower heat transfer coefficient of boiling in this region compared to that at higher heat fluxes. For heat fluxes higher than 65 kW/m², the energy balance closes within 3%. These results indicate that for the lower heat fluxes, relatively more heat losses are present and there is a higher relative uncertainty on the heat flux from the boiling surface to the refrigerant.

B. Heat flux distribution

In the power module, heat is dissipated in the IGBTs. The dissipated heat is transferred to the power module copper baseplate, which acts as a heat spreader, as the IGBTs occupy an area significantly smaller than the baseplate area. To analyse if the heat is uniformly spread over the boiling surface, the boiling phenomenon is visually inspected. The onset of nucleation occurs at the boiling surface edges and random locations on the boiling surface. With increasing heat flux, the nucleation sites spread evenly of the boiling surface. Both for the onset of nucleation and throughout of the nucleate boiling regimes up to critical heat flux, bubble and vapour generation

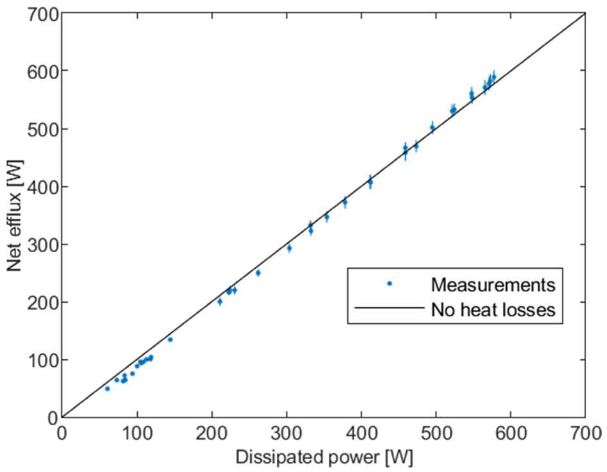

Fig. 4. Net efflux of energy as a function of dissipated power in the power module.

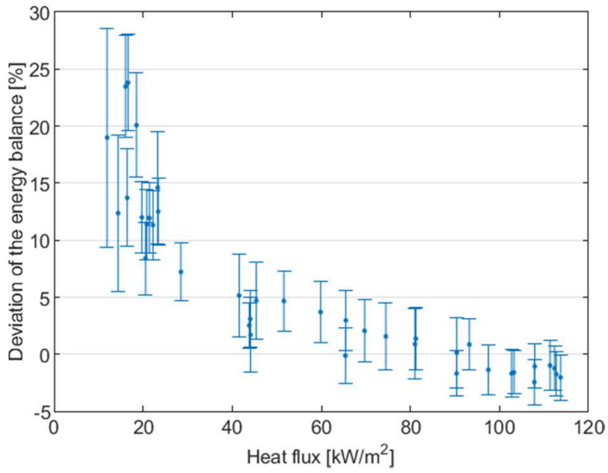

Fig. 5. Relative deviation of the energy balance as a function of the heat flux (electrical power divided by boiling surface area).

occurs uniformly on the boiling surface. No regions of more vigorous vapour generation coinciding with the location of the IGBTs were perceived. From these observations, it is concluded that a quasi-uniform heat flux is present at the boiling surface. This is of importance for the design of pool boiling cooling systems for power modules, as there are no local hot spots and the existing correlations for uniform heat flux are applicable.

C. Boiling Curve

Fig. 6 shows the measured boiling curve. All markers indicate measurement points of nucleate boiling, measurement of natural convection are not included in the figure. The cross markers indicate transition to critical heat flux (CHF). In the boiling curve, the three different zones with different slopes can be clearly distinguished. The initial zone with lower slope lasts up to heat fluxes around 20 kW/m². The second zone, where the slope of the boiling curve is significantly higher, ranges from 20 kW/m² to about 90 kW/m². For even higher heat fluxes, the slope of the boiling curve starts to decrease again until the maximum heat flux is reached.

These three zones are also clearly visible in Fig. 7, which shows the boiling curve with the superheat temperature and heat flux on logarithmic axes. The entire boiling curve cannot be fully correlated by a single power-law equation, as this would result in straight line on a log-log plot as in Fig. 7. The three regimes can be represented by three power-law relations, which are fitted to the measurement data and shown in the figure. In the partial nucleate boiling region, heat flux varies with the surface superheat temperature raised to the power 1.36. This power corresponds well to the power found in natural convection heat transfer, indicating enhanced natural convection may be the dominant heat transfer mechanism in this region. A far steeper rise in heat flux with surface superheat temperature is measured in the fully developed boiling region, heat flux varies with surface superheat raised to a power of 5.29. For higher heat fluxes closer to CHF, in the partial dryout region, surface superheat temperatures increase more with heat flux than for the fully developed boiling region. The relation between heat flux and surface superheat is best correlated by a power-law with a power equal to 1.07, which indicates an almost linear relation between heat

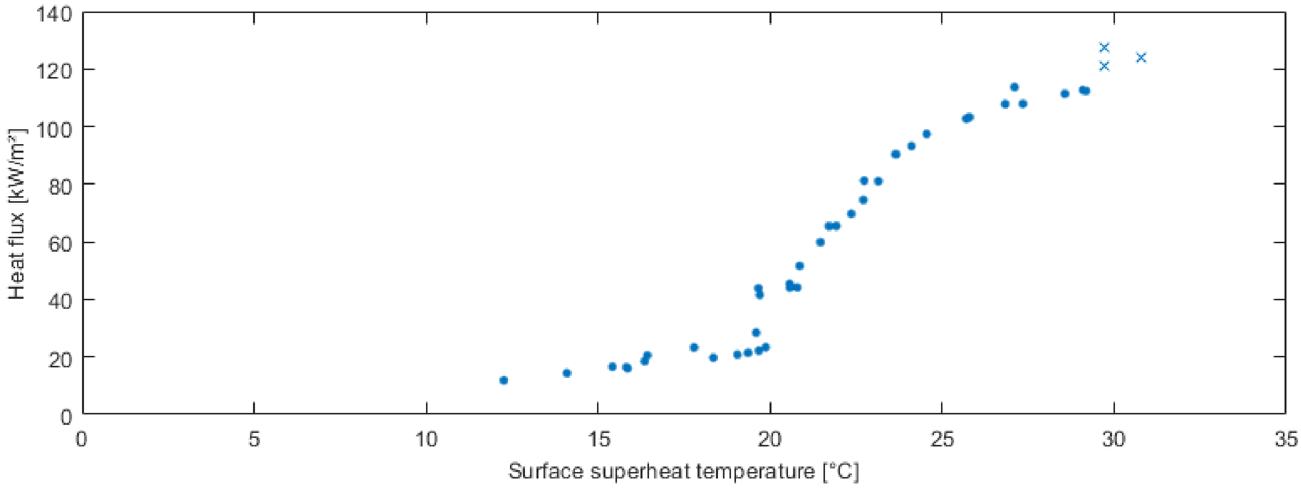

Fig. 6. Boiling curve of FK-649 at saturation temperature 36 °C, cross markers indicate CHF.

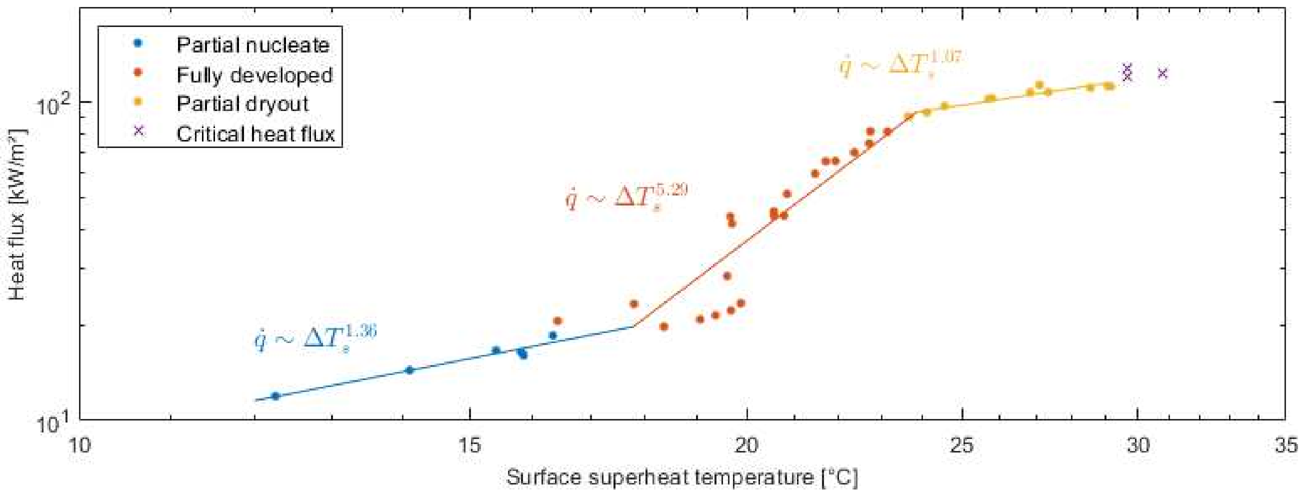

Fig. 7. Boiling curve of FK-649 at saturation temperature 36°C on a plot with logarithmic axes with the three nucleate boiling regimes indicated.

flux and surface superheat temperature. The curves on Fig. 7 as given by equations (2), (3) and (4) for respectively the partial nucleate boiling regime, the fully developed nucleate boiling regime and the partial dryout regime.

$$\dot{q} = 389\ \Delta T_s^{1.36} \tag{2}$$

$$\dot{q} = 0.00489\ \Delta T_s^{5.29} \tag{3}$$

$$\dot{q} = 3178\ \Delta T_s^{1.07} \tag{4}$$

These measurements indicate a single power-law relation between heat flux and surface superheat temperature is not sufficient to accurately predict the boiling curve for FK-649. Further measurements with more saturation temperatures and other fluids should be performed to analyse if this behaviour is universally valid.

IV. Conclusion

This paper reports on measurements of nucleate pool boiling heat transfer from a power module baseplate to refrigerant FK-649. The boiling curve exhibits a different behaviour in three different zones: partial nucleate boiling (below 20 kW/m²), fully developed nucleate boiling (from 20 kW/m² to 90 kW/m²) and partial dryout nucleate boiling (90 kW/m² to CHF). A single power-law relation between heat flux and surface superheat temperature, which is used by most correlations, is not sufficient to accurately described the boiling curve. A combination of three power-law relations is fitted to the measured boiling curve to represent the three zones.

References

[1] R. C. Chu, "The Challenges of Electronic Cooling: Past, Current and Future," *J. Electron. Packag.*, vol. 126, no. 4, pp. 491–500, Jan. 2005, doi: 10.1115/1.1839594.

[2] N. Kattan, J. R. Thome, and D. Favrat, "Flow Boiling in Horizontal Tubes: Part 3—Development of a New Heat Transfer Model Based on Flow Pattern," *J. Heat Transf.*, vol. 120, no. 1, pp. 156–165, Feb. 1998, doi: 10.1115/1.2830039.

[3] V. K. Dhir, "Boiling Heat Transfer," *Annu. Rev. Fluid Mech.*, vol. 30, no. 1, pp. 365–401, 1998.

[4] S. G. Kandlikar and J. N. Chung, "Boiling and Condensation," in *Multiphase flow handbook*, C. T. Crowe, Ed. Boca Raton, FL: CRC : Taylor & Francis, 2006, pp. 131–190.

[5] M. S. El-Genk and H. Bostanci, "Saturation boiling of HFE-7100 from a copper surface, simulating a microelectronic chip," *Int. J. Heat Mass Transf.*, vol. 46, no. 10, pp. 1841–1854, May 2003, doi: 10.1016/S0017-9310(02)00489-1.

[6] S. S. Kutateladze, "Natural Convection Boiling of Pure Saturated Fluids," in *Heat Transfer and Hydrodynamic Resistance: Handbook*, 1990, pp. 197–200.

[7] E. C. Forrest, L.-W. Hu, J. Buongiorno, and T. J. McKrell, "Pool Boiling Heat Transfer Performance of a Dielectric Fluid With Low

Global Warming Potential," *Heat Transf. Eng.*, vol. 34, no. 15, pp. 1262–1277, Dec. 2013, doi: 10.1080/01457632.2013.793103.
[8] W.-T. Ji, C.-Y. Zhao, Y.-L. He, and W.-Q. Tao, "Experimental validation of Cooper correlation at higher heat flux," *Int. J. Heat Mass Transf.*, vol. 90, pp. 1241–1243, Nov. 2015, doi: 10.1016/j.ijheatmasstransfer.2015.05.107.
[9] R. S. Bartle, K. Menon, and E. Walsh, "Pool boiling of resin-impregnated motor windings geometry," *Appl. Therm. Eng.*, vol. 130, pp. 854–864, Feb. 2018, doi: 10.1016/j.applthermaleng.2017.11.053.
[10] G. Kruzhilin, "Free-convection transfer of heat from a horizontal plate and boiling liquid," *Dokl. SSSR Rep. USSR Acad. Sci.*, vol. 58, no. 8, pp. 1657–1660, 1947.
[11] W. Rohsenow, "A Method of Correlating Heat-Transfer Data for Surface Boiling Liquids," *Trans. ASME*, vol. 74, no. 6, pp. 969–976, 1952.
[12] H. K. Forster and N. Zuber, "Dynamics of vapor bubbles and boiling heat transfer," *AIChE J.*, vol. 1, no. 4, pp. 531–535, Dec. 1955, doi: 10.1002/aic.690010425.
[13] S. S. Kutateladze and V. M. Borishanskii, *Handbook on Heat Transfer*. 1958.
[14] V. M. Borishanskii, "Accounting for the Effect of Pressure on Heat Transfer and Critical Heat Flux during Boiling Using the Theory of Thermodynamic Similarity," in *Problems of Heat Transfer and Hydraulics in Two-Phase Media*, S. S. Kutateladze, Ed. 1961, pp. 18–36.
[15] V. M. Borishanskii, "Correlation of the Effect of Pressure on the Critical Heat Flux and Heat Transfer Rates Using the Theory of Thermodynamic Similarity," in *Problems of Heat Transfer and Hydraulics of Two-Phase Media*, S. S. Kutateladze, Ed. Pergamon, 1969, pp. 16–37. doi: 10.1016/B978-0-08-012077-5.50008-7.
[16] I. Shekriladze and G. Ratiani, "On the basic regularities of developed nucleate boiling heat transfer," *Bull Acad Sci Georg SSR*, vol. 42, no. 1, pp. 145–150, 1966.
[17] I. G. Shekriladze, "Developed boiling heat transfer," *Int. J. Heat Mass Transf.*, vol. 24, no. 5, pp. 795–801, May 1981, doi: 10.1016/S0017-9310(81)80002-6.
[18] D. A. Labuntsov, "Heat Transfer Problems with Nucleate Boiling of Liquids," *Teploenergetika*, vol. 19, no. 9, pp. 21–28, 1972.
[19] D. Gorenflo, P. Sokol, and S. Caplanis, "Pool boiling heat transfer from single plain tubes to various hydrocarbons," *Int. J. Refrig.*, vol. 13, no. 5, pp. 286–292, Sep. 1990, doi: 10.1016/0140-7007(90)90059-6.
[20] D. Gorenflo and D. Kenning, "Pool Boiling," in *VDI Heat Atlas*, 2nd ed., P. Stephan, Ed. Berlin, Heidelberg: Springer Berlin Heidelberg, 2010, pp. 757–792. doi: 10.1007/978-3-540-77877-6.
[21] K. Stephan and M. Abdelsalam, "Heat-transfer correlations for natural convection boiling," *Int. J. Heat Mass Transf.*, vol. 23, no. 1, pp. 73–87, Jan. 1980, doi: 10.1016/0017-9310(80)90140-4.
[22] M. G. Cooper, "Heat Flow Rates in Saturated Nucleate Pool Boiling-A Wide-Ranging Examination Using Reduced Properties," in *Advances in Heat Transfer*, vol. 16, J. P. Hartnett and T. F. Irvine, Eds. Elsevier, 1984, pp. 157–239. doi: 10.1016/S0065-2717(08)70205-3.
[23] W. Leiner, "Heat transfer by nucleate pool boiling—general correlation based on thermodynamic similarity," *Int. J. Heat Mass Transf.*, vol. 37, no. 5, pp. 763–769, Mar. 1994, doi: 10.1016/0017-9310(94)90114-7.
[24] I. L. Pioro, W. Rohsenow, and S. S. Doerffer, "Nucleate pool-boiling heat transfer. II: assessment of prediction methods," *Int. J. Heat Mass Transf.*, vol. 47, no. 23, pp. 5045–5057, Nov. 2004, doi: 10.1016/j.ijheatmasstransfer.2004.06.020.
[25] I. H. Bell, J. Wronski, S. Quoilin, and V. Lemort, "Pure and Pseudo-pure Fluid Thermophysical Property Evaluation and the Open-Source Thermophysical Property Library CoolProp," *Ind. Eng. Chem. Res.*, vol. 53, no. 6, pp. 2498–2508, Feb. 2014, doi: 10.1021/ie4033999.